


PAPER

[View Article Online](#)
[View Journal](#) | [View Issue](#)Cite this: *Catal. Sci. Technol.*, 2021, 11, 2461

Engineering the large pocket of an (S)-selective transaminase for asymmetric synthesis of (S)-1-amino-1-phenylpropane†

Youyu Xie,^a Feng Xu,^a Lin Yang,^a He Liu,^a Xiangyang Xu,^b
Hualei Wang ^{*a} and Dongzhi Wei ^{*a}

Amine transaminases offer an environmentally benign chiral amine asymmetric synthesis route. However, their catalytic efficiency towards bulky chiral amine asymmetric synthesis is limited by the natural geometric structure of the small pocket, representing a great challenge for industrial applications. Here, we rationally engineered the large binding pocket of an (S)-selective ω -transaminase BPTA from *Paraburkholderia phymatum* to relieve the inherent restriction caused by the small pocket and efficiently transform the prochiral aryl alkyl ketone 1-propiophenone with a small substituent larger than the methyl group. Based on combined molecular docking and dynamic simulation analyses, we identified a non-classical substrate conformation, located in the active site with steric hindrance and undesired interactions, to be responsible for the low catalytic efficiency. By relieving the steric barrier with W82A, we improved the specific activity by 14-times compared to WT. A π - π stacking interaction was then introduced by M78F and I284F to strengthen the binding affinity with a large binding pocket to balance the undesired interactions generated by F44. T440Q further enhanced the substrate affinity by providing a more hydrophobic and flexible environment close to the active site entry. Finally, we constructed a quadruple variant M78F/W82A/I284F/T440Q to generate the most productive substrate conformation. The 1-propiophenone catalytic efficiency of the mutant was enhanced by more than 470-times in terms of k_{cat}/K_M , and the conversion increased from 1.3 to 94.4% compared with that of WT, without any stereoselectivity loss (ee > 99.9%). Meanwhile, the obtained mutant also showed significant activity improvements towards various aryl alkyl ketones with a small substituent larger than the methyl group ranging between 104- and 230-fold, demonstrating great potential for the efficient synthesis of enantiopure aryl alkyl amines with steric hindrance in the small binding pocket.

Received 19th December 2020,
Accepted 28th January 2021

DOI: 10.1039/d0cy02426k

rsc.li/catalysis

Introduction

Approximately 95% of drugs are predicted to be chiral by 2020 and share a market of almost \$5b in chiral ligands and agrochemicals.^{1,2} Chiral amines play a fundamental role in a series of pharmaceutical drugs, and approximately 40% of them are estimated to contain a chiral amine functionality.³ The asymmetric synthesis of chiral amine drug intermediates by enzymatic catalysis strategies has attracted growing attention due to the social and environmental demand for green processes in the chemical industry.^{4–6} Transaminases

present stringent stereoselectivity, no requirement of external cofactor supplementation, a broad substrate spectrum, and high stability, which makes them attractive for industrial process development.^{7–9}

Transaminases require pyridoxal 5'-phosphate (PLP) as a coenzyme that mediates the transamination of prochiral keto acids or ketones by transferring an amine group from an amino donor.¹⁰ The active site of (S)-selective transaminases is composed of a small and a large binding pocket (SBP and LBP, respectively) in the dimerization of monomers.¹¹ In most cases, the large pocket can accommodate substituents with a rather broad size distribution,¹² while the small pocket is restricted to accept only a methyl group.¹³ The steric constraint in the active site, especially that in the SBP, has been the crucial limiting factor for the production of various bulky chiral amines, representing a great challenge for industrial synthetic applications.

To boost the synthesis utility of ω -TAs toward bulky prochiral ketones, protein engineering has been widely

^a State Key Laboratory of Bioreactor Engineering, New World Institute of Biotechnology, East China University of Science and Technology, Shanghai 200237, People's Republic of China. E-mail: hlwang@ecust.edu.cn, dzhwei@ecust.edu.cn

^b Zaozhuang Jienuo Enzyme Co., Ltd., Shandong Province 277116, PR China

† Electronic supplementary information (ESI) available. See DOI: 10.1039/d0cy02426k

carried out to overcome the limitation of the binding pocket geometry by using directed evolution and semi-rational/rational design approaches for different amine transaminases.^{14,15} An impressive example was highlighted by Merck and Co. and Codex, applying the direct evolution of an (*R*)-selective ω -transaminase ATA-117 for enlarging the LBP and SBP to the highly efficient asymmetric synthesis of bulky chiral sitagliptin.¹⁴ Regarding rational (*S*)-TA engineering, most studies focused on engineering the LBP and SBP to modify the acceptance of bulky substrates. Dourado *et al.*¹⁶ engineered the LBP and SBP of the transaminase *Vibrio fluvialis* TAM and achieved a high catalytic activity for the chiral synthesis of (1*S*)-1-(1,1'-biphenyl-2-yl)ethanolamine. Midelfort *et al.*¹⁷ engineered the LBP and SBP of *Vibrio fluvialis* TAM and improved the catalytic conversion of (*R*)-ethyl-5-methyl-3-oxooctanoate by 60-times. Han *et al.*¹⁸ expanded the bulky substrate specificity for aryl alkylamines and alkylamines of ω -transaminase OATA by rational LBP remodeling. However, successful examples of SBP engineering to accommodate bulky substrates are still needed to be developed.^{15,18–24} Most residues in the SBP were adjacent to PLP and stayed at the interface of the homodimer, which played an important role in the stabilization and stereoselectivity of the ω -transaminase. In most cases, modifying the residues in the SBP would result in catalytic activity loss toward prochiral ketones.²⁵ Therefore, it is rather difficult to improve the catalytic efficiency for aryl alkyl substrates with alkyl chains larger than a methyl group by engineering the SBP.

In this study, we rationally engineered the LBP of an (*S*)- ω -transaminase BPTA from *Paraburkholderia phymatum* to address the challenge of aryl alkyl substrates being generally hardly accommodated in the SBP by relieving steric hindrance and strengthening the interaction upon substrate binding in the LBP.

Results and discussion

Initial screening of ω -transaminases

Although transaminases have a broad substrate range, most of them accept only substituents no larger than a methyl group at the position adjacent to the carbonyl moiety of the ketone substrate.¹⁴ To identify a potential candidate for the asymmetric synthesis of bulky chiral pharmaceutical intermediates, we selected (*S*)-1-amino-1-phenylpropane (**1b**) (precursor of corticotropin-releasing factor type I antagonist) as the model substrate for initial screening, which is generally difficult to accommodate by the SBP of most ω -transaminases due to the small ethyl group substituent of the prochiral ketone. A total of 72 in-house natural ω -TAs (not supplied) were screened in the thermodynamically favored kinetic mode using an (*S*)-amine as a donor and pyruvate as an acceptor. The results showed that only one constructed ω -transaminase BPTA from *Paraburkholderia phymatum* STM815 (accession number: WP_012402885.1) could be determined with poor detectable activity, and the

conversion of the target ketone **2b** (10 mM) was only 1.3% at 48 h, indicating that the ethyl group of the model substrate was indeed not easily accommodated by the ω -transaminase SBP due to the limitation of the natural SBP geometry.

Molecular modeling of the BPTA active site

Molecular docking and MD simulations were performed to analyze the interaction between the ketone and the residues in the active site. We used the ω -transaminase crystal structure with the PMP cofactor from *Chromobacterium violaceum* (PDB ID: 6s4g)²⁶ with 58.84% identity as a template for comparative modeling. The substrate **2b** was docked into the BPTA active site with the PMP cofactor, and the top-ranked structure with the lowest binding energy was chosen as the initial conformation for the MD simulation (Fig. 1A). During 50 ns of MD simulation, the result showed that the substrate could not form a stable attack conformation in the active site and would move out of the BPTA active site after 8.3 ns. The distance between the PMP's exocyclic nitrogen and the ketone's carbonyl carbon atom (d1) showed two major increases from 0 to 8.3 ns and 8.3 to 47.4 ns. The first increase occurred at 8.3 ns, where d1 increased to 7.5 Å, and the second increase at 47.4 ns with d1 sharply increasing to >10.0 Å (Fig. 1A). This phenomenon was similar to that described by Voss *et al.*¹³ and indicated that the pocket in the active site of BPTA failed to generate sufficient affinity to stabilize the Michaelis complex between the ketone and PMP,²⁷ which was necessary to activate the transamination catalysis. The conformation before 8.3 ns in the MD simulation represents a plausible attack conformation that could initiate external aldimine formation. Therefore, we extracted the average structure before 8.3 ns in the MD simulation for subsequent analysis.

Rational design of the large pocket of the active site

Based on the modeling results, the small BPTA binding pocket consisted of F44, L81, F110, Y175, and G341, while the large one was constructed by M78, W82, A253, I284, R438, and T440 (Fig. S2†). As Scheme 1 shows, the classical nucleophilic attack conformation indicated that a small substituent of the ketone is located in the SBP and the large substituent adjacent to the carbonyl group stayed in the LBP. However, the docking results showed a non-classical substrate conformation in the active site, with the phenyl moiety pointing out of the LBP, while the small substituent pointed towards the LBP (Fig. 1A). This non-classical conformation seemed to be the main reason for the low catalytic activity towards the model substrate.^{13,28}

The interactions between the substrate and residues in the active site were analyzed to further explore the reason for the abnormal conformation mentioned above. As shown in Fig. 1B, the indole moiety of W82 showed a huge steric hindrance with ketones, which hampered their efficient binding to the SBP and LBP in the active site. Meanwhile, the side chain of F44 generated an undesired π - π stacking

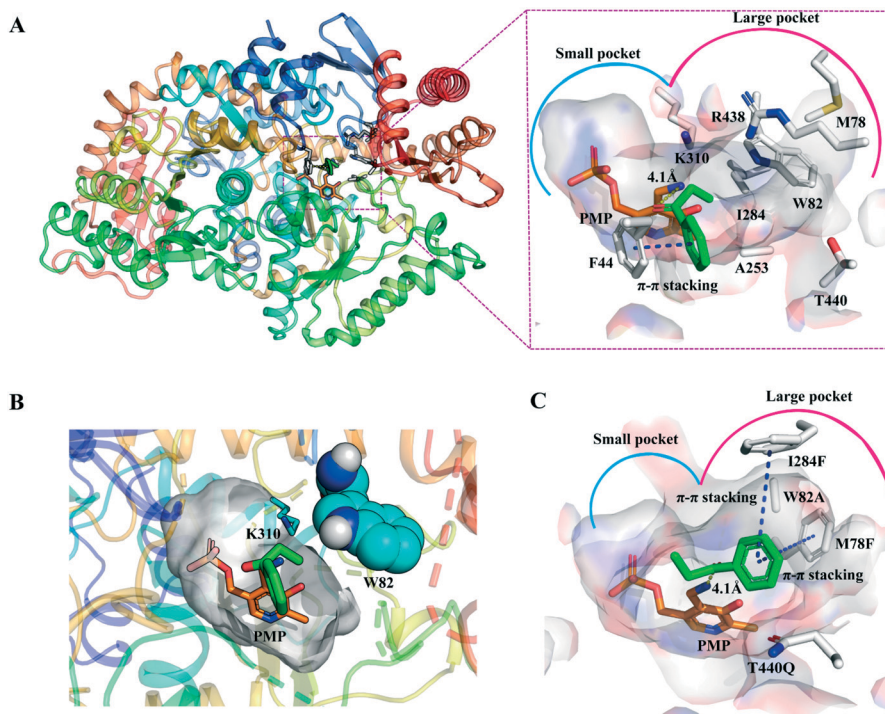
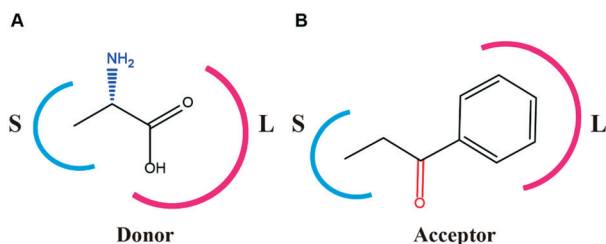


Fig. 1 Docking model of 1-propiofenone in the BPTA active site. (A) The residues of the active site in the docking model. The green and orange sticks represent the substrate ketone and PMP, respectively. The yellow dotted line between the exocyclic nitrogen of PMP and the carbonyl carbon atom of the ketone represents the distance. The brown dotted line between the phenyl group of F44 and the phenyl moiety of the substrate represents the π - π stacking interaction between them. (B) Side view of the ketone substrate phenyl group interaction visualization with the W82 indolyl group, shown as a blue CPK representation. The yellow dotted line represents the distance between the exocyclic nitrogen of PMP and the carbonyl carbon atom of the ketone. Orange sticks indicate the internal aldimine. (C) White, orange, and green sticks indicate the key mutation residues in the docking conformation of variant W82A/M78F/I284F/T440Q, the internal aldimine, and the ketone, respectively.

interaction with the ketone, and the stacking interaction prevented the phenyl group from being properly accommodated in the LBP. We speculated that the steric hindrance of W82 and undesired interaction of F44 with the substrate might result in poor catalytic efficiency (Fig. 1A).

To alleviate the steric hindrance and maintain the hydrophobic environment at the same time, hydrophobic and smaller substituents (FLIVAG) were selected to replace the W82 residue with the phenyl group. The results showed that there are two positive mutations W82L and W82A with

better catalytic activity, improving by 3.89 and 14.00-times in $k_{\text{cat}}/K_{\text{M}}$ compared to WT (Table 1), respectively. Both variants showed a sharply decreased K_{M} . Among them, the K_{M} value of W82A decreased from 92.86 to 11.00 mM, demonstrating significant improvement in affinity with the substrate by the W82A mutation. Considering that F44 in the SBP was at the interface of the dimer, there was no particular rule to modify this position, and the saturated mutation of F44 was carried out. Unfortunately, the saturation mutations at F44 showed no positive results compared to WT towards **2b**, and most of the variants showed no detectable catalytic activity (Fig. S3†). This result indicated that it would be critical to engineer the position at the interface, which is correlated to enzyme stability and enantioselectivity.¹³ To eliminate the unfavorable interaction produced by F44 in the SBP, the residues in the LBP (M78, W82, A253, I284, R438, and T440) in the opposite direction (LBP) were investigated for their potential in improving the binding interaction with the phenyl group of the ketone in the LBP. Among them, residue R438 plays an important role in dual substrate recognition, and is responsible for forming a salt bridge with the carboxylate group of the donor and acceptor substrate,²⁹ while A253 participates in the binding of PLP.^{30,31} Therefore, these two conserved sites were excluded from our consideration for modification.



Scheme 1 The classical substrate binding conformation in the active site using L-Ala as an amine donor and 1-propiofenone as a bulky ketone acceptor, as a model. (A) Binding of the amine donor L-Ala to the PLP form of the ω -TAs (E-PLP). (B) Binding of the substrate ketone acceptor 1-propiofenone to the pyridoxamine 5'-phosphate form of the ω -TAs (E-PMP).

Table 1 Kinetic parameters towards 1-propiophenone in kinetic resolution mode

Variant	K_M [mM]	k_{cat} [s^{-1}]	k_{cat}/K_M [$M^{-1} s^{-1}$]	Fold increase in k_{cat}/K_M
BPTA-WT	92.86 \pm 2.16	0.68 \pm 0.03	7.27 \pm 0.17	1.00
W82A	11.00 \pm 0.24	1.12 \pm 0.07	101.82 \pm 5.59	14.01
W82L	30.10 \pm 1.17	0.85 \pm 0.01	28.29 \pm 2.36	3.89
W82A/M78F	4.90 \pm 0.44	3.31 \pm 0.04	681.07 \pm 16.99	93.70
W82A/I284F	6.00 \pm 0.59	1.73 \pm 0.15	288.33 \pm 5.63	39.67
W82A/T440Q	7.94 \pm 0.26	1.37 \pm 0.05	172.54 \pm 4.38	23.74
M78F/W82A/I284F	3.14 \pm 0.19	4.92 \pm 0.78	1566.88 \pm 48.69	215.56
W82A/I284F/T440Q	5.32 \pm 0.93	1.96 \pm 0.14	368.42 \pm 14.43	50.68
M78F/W82A/T440Q	3.48 \pm 0.48	4.42 \pm 0.33	1270.11 \pm 12.21	174.73
M78F/W82A/I284F/T440Q	1.67 \pm 0.11	5.71 \pm 0.54	3419.16 \pm 45.63	470.38

The residues M78 and I284 were located directly opposite to F44 (Fig. 1A). We speculated that introducing an opposite π - π stacking interaction would be helpful for the phenyl substituent of the substrate binding in the LBP. Thus, we replaced M78 and I284 with hydrophobic and aromatic substituents (WF) using W82A as a template to construct double variants. The mutation results showed that the catalytic efficiency of W82A/M78F and W82A/I284F increased by 93.07 and 39.67-times (Table 1) in terms of k_{cat}/K_M compared to that of WT, respectively. The K_M values of W82A/M78F and W82A/I284F decreased by 19.10-times and 15.47-times relative to that of WT, respectively. The lower K_M and significant improvement in the k_{cat} values of W82A/M78F and W82A/I284F demonstrated that the introduced π - π stacking interaction was important to enhance the affinity with the phenyl group of the substrate and to improve the catalytic efficiency.

The residue T440 was located in a flexible loop, close to the entrance of the active site (Fig. 2). Considering the polar property of T440, which may prevent the diffusion of the hydrophobic substrate into the active site, a relatively more flexible and (or) less sterically hindered residue than T440

may be advantageous for improving affinity and maintaining the flexible property of the loop for efficient diffusion of the bulky substrate. According to the hydropathy index of 20 amino acids,³² arginine, lysine, and histidine are basic amino acids, while glutamic acid and aspartic acid are acidic amino acids, all of which should be excluded for its strongest hydropathy index of the side chains. Then, a smart library (MILVACNQ) was constructed based on W82A and the mutation results showed that only one mutant W82A/T440Q exhibited positive catalytic activity with a 23.74-fold improvement (Table 1) in k_{cat}/K_M compared to WT. Compared with other residues included in the smart library (MILVACN) constructed, residue Q may occupy more space; however, it was the most flexible residue among them. We speculated that the flexible property of Q440 was more helpful for substrate diffusion than for relieving steric hindrance. The results indicated that the diffusion of the substrate in the active site played a key role in the catalytic activity of the ω -TA enzymes.

Based on the above results, four sites were identified to be responsible for the catalytic activity of BPTA, and the mutant obtained demonstrated improved catalytic activity towards the substrate ketone. Considering the potential positive additive effects between these positive mutations, triple and quadruple iterative combinatorial mutageneses were carried out to further improve the enzyme activity of BPTA. The results of the mutation are summarized in Table 1. The results showed that all the variants presented positive synergistic effects among the selected residues. Among them, the best triple mutant was M78F/W82A/I284F with a 215.56-fold increase in k_{cat}/K_M relative to that of WT, while the most effective variant obtained was quadruple mutant M78F/W82A/I284F/T440Q, which sharply increased enzyme activity by 470.38-times in terms of k_{cat}/K_M compared to WT, exhibiting commendably positive additive effects. The K_M value of W82A/M78F/I284F/T440Q significantly decreased from 92.86 to 1.67 mM, which indicated that W82A/M78F/I284F/T440Q sharply promoted the affinity with the substrate ketone.

Molecular dynamics (MD) simulation was applied to interpret the interaction between the variants and the substrate (Fig. S4†). The complex of variant W82A and the substrate ketone was investigated during a 50 ns MD simulation. Despite the distance fluctuation between the ketone and PMP during MD simulation, the ketone remained

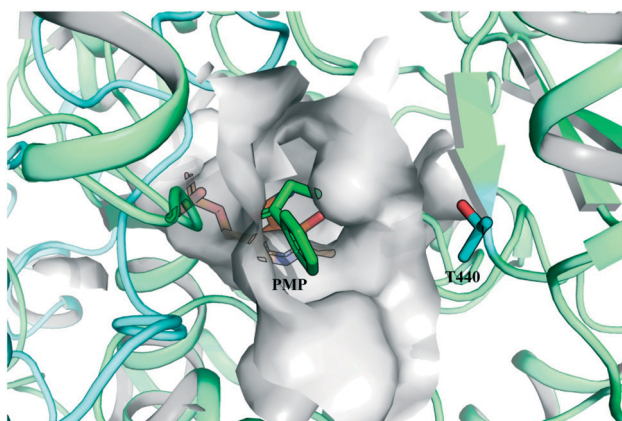


Fig. 2 A perspective of T440 in the active site. The structure of the enzyme is represented by a rainbow-colored cartoon, the substrate binding pocket is represented by a white-colored surface, and the cofactor PMP and the substrate are represented by orange and green sticks, respectively. The residues in position T440 are represented by blue sticks.

stable in the active site, and the average distance d_1 was 5.7 Å compared to 6.4 Å of WT during the MD simulation (Fig. S5A and B†). This indicated that by relieving the steric hindrance by the smaller hydrophobic substituent, the capacity to accommodate the phenyl group increased. In addition, the MMPBSA-based binding free energy ($\Delta\Delta G_{W82A}$)³³ was calculated to be $-3.42 \text{ kcal mol}^{-1}$ compared to $1.24 \text{ kcal mol}^{-1}$ for WT, demonstrating an increased affinity for the substrate ketone. These results were in line with the kinetic analysis. The complex conformation of variant M78F/W82A/I284F/T440Q during MD simulation showed that the substrate ketone was stable in the active site and the average distance between the PMP's exocyclic nitrogen and the ketone's carbonyl carbon atom was 4.86 Å, which was closer to the PMP's exocyclic nitrogen. Significantly, the phenyl and alkyl groups of the substrate were beneficially accommodated in the large pocket and small pocket (Fig. S5C†) in the right form of the classical Michaelis complex as described by Cassimjee *et al.*,²⁷ which was helpful for a nucleophilic attack between PMP's exocyclic nitrogen and the ketone's carbonyl carbon atom in the transaminase. As shown in Fig. 1C, the side chains of M78F and I284F pointed towards the phenyl group of the substrate and formed a tractive π - π stacking interaction with the phenyl group, which further strengthened the interaction with the phenyl group to pull it appropriately back to the LBP. In addition, the $\Delta\Delta G_{W82A/M78F/I284F/T440Q}$ value was $-36.33 \text{ kcal mol}^{-1}$, which indicates that W82A/M78F/I284F/T440Q indeed improved the affinity with the substrate and finally remodeled the conformation into a productive conformation with the ethyl group normally accommodated in the SBP and the phenyl group positioned in the LBP.

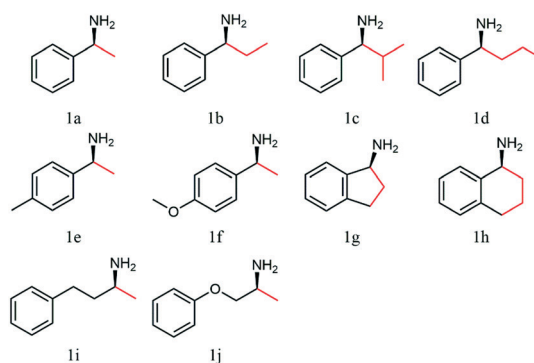
By combining molecular docking and MD simulation analysis, the key mutations (M78F, W82A, I284F and T440Q) of BPTA were identified to be responsible for accommodating aryl alkyl substrates, and they were all located in the LBP of the active site. At present, many significant advances have been achieved by engineering (S)-selective TAs for bulky substrates.^{12,13,15,16,20,34,35} For example, Pavlidis *et al.*¹⁵ have successfully obtained an (S)-selective TA mutant Y59W/Y87F/Y152F/P423H from *Ruegeria sp.* TM1040, which showed an 8900-fold improvement towards the bulky substrate (S)-1,3-diphenylpropan-1-amine. Nobili *et al.*¹² identified two mutants (F85L/V153A and Y150F/V153A) from *Vibrio fluvialis* showing a 30-fold increased activity in the conversion of (S)-phenylbutylamine and (R)-phenylglycinol, respectively. Voss *et al.*¹³ obtained two double mutants (F88L/C418(G/L)) from *Chromobacterium violaceum* which showed >200-fold improved activities in the conversion of 1-phenylbutylamine. Most of the engineering studies on TAs were focused on modifying the LBP and SBP. The modification studies mentioned above modified either both the LBP and SBP or only the SBP to achieve the enhancement of the catalytic efficiency towards bulky substrates. In contrast, we reshaped the LBP to improve the conversion efficiency towards the SBP accommodating aryl alkyl substrates. In order to explore the

differences of the amino acid locations in the LBP between those in the engineering studies and BPTA in our study, multiple amino acid sequence alignment was performed (Table S2 and Fig. S6†).³⁶ The result showed that BPTA shared relatively small similarities with the TAs with 37.1% (*Ruegeria sp.* TM1040), 33.9% (*Vibrio fluvialis*) and 62.2% similarity (*Chromobacterium violaceum*), respectively. Three of the four mutations identified in our study shared similar locations with the TAs mentioned above, such as W82 in 3FCR (corresponding to Y59), W82 and I284 in 4E3Q (corresponding to W57 and I259, respectively), and T440 in 4A6R (corresponding to C418) (Fig. S6†), demonstrating that these locations are hotspots in engineering (S)-TAs for accommodating bulky substrates. However, the mutated residues obtained in our study were basically different from those of the TAs referred above. Due to the diverse substrates employed, it was hard to exactly predict the positive residues to be mutated in a given situation. Except for the three similar locations, M78 was a new hotspot identified in our study which was not reported before. Among the three double mutants constructed on the base of W82A (Table 1), the mutant W82A/M78F showed the highest activity with up to 6.7 fold improvement compared to W82A. Meanwhile, W82A/I284F and W82A/T440Q gave a 2.9 and 1.7-fold improvement, respectively. This newly identified residue M78 may be a potential hotspot in engineering TAs for accommodating aryl alkyl substrates.

Activity improvements towards bulky substrate analysis

To explore the synthetic and deracemization utility of BPTA_{M78F/W82A/I284F/T440Q} for bulky substrates, the catalytic activities toward aryl alkyl amines (compounds 1, using '1' as a prefix, such as '1a, 1b, 1c...') (Scheme 2) and corresponding ketones (compounds 2, using '2' as a prefix, such as '2a, 2b, 2c...') were investigated using pyruvic acid as the acceptor and L-Ala as the amine donor, respectively.

The kinetic resolution results showed that WT exhibited modest catalytic activity toward the majority of the bulky amines, with which the aryl moiety was generally



Scheme 2 Chiral amine donors used in this study.

Table 2 Activity improvements of BPTAM78F/W82A/I284F/T440Q towards various amines in kinetic resolution mode

Amines	Relative reactivity ^a [%]		Fold-increase
	BPTA	BPTA _{M78F/W82A/I284F/T440Q}	
1a	100.00 ^b	118.42 ± 4.44	1.18
1b	8.89 ± 0.34	92.98 ± 2.11	10.46
1c	2.13 ± 0.18	19.10 ± 1.12	8.97
1d	2.25 ± 0.06	16.52 ± 3.21	7.34
1e	76.53 ± 1.56	95.03 ± 1.66	1.24
1f	114.48 ± 2.35	116.69 ± 5.55	1.02
1g	84.38 ± 1.36	112.28 ± 3.38	1.33
1h	74.12 ± 3.54	104.05 ± 8.74	1.40
1i	98.42 ± 2.37	127.51 ± 1.11	1.30
1j	117.13 ± 5.56	114.05 ± 6.18	0.97

^a The relative activity was determined from the initial reaction rate (*i.e.*, conversion <10%) compared with that of the WT enzyme. The reaction conditions were as follows: 15% DMSO, 50 mM amine donor, 50 mM pyruvic acid, and 0.2 μM purified enzyme in 100 mM Tris-HCl buffer (pH = 8.0) containing 0.1 mM PLP at 30 °C for 10 min; analyzed using HPLC. ^b The initial reaction rate was 386.9 μM min⁻¹.

accommodated in the LBP (Table 2). However, when the length of the alkyl chain of the substrates was longer than that of the methyl group (**1b**, **c**, and **d**), WT showed poor catalytic performance with a minimum relative activity as low as 2.13% compared to **1a**. In contrast, the variant M78F/W82A/I284F/T440Q showed a substantial improvement in activity toward most of the substrates except **1j** (0.97-fold). Intriguingly, the mutant presented sharp catalytic improvements towards bulky amines with longer alkyl chains: **1b** (10.46-fold), **1c** (8.97-fold), and **1d** (7.34-fold), which indicated that engineering the LBP of the enzyme improved the catalytic activity toward bulky amines, especially aryl alkyl amines with long alkyl chains.

The specific activities toward aryl alkyl ketones were investigated and showed a similar trend compared to the catalytic activity improvements in resolution mode (Table 2). WT showed relatively higher activity for **2e**, **2f**, **2i**, and **2j**; these substrates were all aryl alkyl ketones with a methyl

group as the small substituent, which indicated that the volume of the LBP of BPTA was large enough to synthetically accommodate the substrate ketones with an aryl group. However, when it comes to bulky substrates with two bulky substituents, such as aryl alkyl ketones (**2b–d**), indanone (**2g**), and tetralone (**2h**), which were aryl substrates with a small substituent bulkier than the methyl group, WT showed decreasing activities ranging from 0.01 to 0.15-fold. It was demonstrated that it is difficult for WT to accommodate aryl alkyl ketones with longer alkyl side chains in the SBP. Fortunately, the variant BPTA_{M78F/W82A/I284F/T440Q} showed significant activity improvements towards the majority of bulky ketones compared to WT (Table 3). Among these aryl alkyl ketones, the variant W82A/M78F/I284F/T440Q showed a sharp improvement in activity for the bulky substrate ketones with two bulky substituents (*i.e.*, 104.0, 230.0, and 224.8-fold reaction increases for **2b**, **c**, and **d**, respectively). This indicated that the mutant W82A/M78F/I284F/T440Q improved the catalytic activity towards aryl alkyl substrates, especially the substrate ketones with longer alkyl side chains that are accommodated in the SBP.

Cascade strategies for chiral amine asymmetric synthesis

As a commonly used amino donor for most transaminases, alanine has been widely used in the asymmetric synthesis of chiral amines.³⁷ However, due to the low equilibrium constant of alanine ($K_{eq} < 10^{-3}$),³⁸ the equilibration problem of the transaminases is the main challenge for industrial process requirements. In addition, the co-product pyruvate generated in the amination process inhibits amine production. Multiple cascade strategies have already been established to efficiently replace the transaminase equilibrium shift.^{39,40} To evaluate the practical utility of variant BPTA_{M78F/W82A/I284F/T440Q} towards the asymmetric synthesis of chiral amine **1b** with L-alanine as an amine donor, we investigated different cascade reaction systems to displace the unfavorable equilibration in the asymmetric synthesis of (*S*)-1-amino-1-phenylpropane. As shown in Fig. 3D, the synthetic efficiency of chiral amine **1b** in all the cascade

Table 3 Activity improvements of BPTAM78F/W82A/I284F/T440Q towards various acceptors

Ketones	Relative reactivity ^a [%]		Fold-increase
	BPTA	BPTA _{M78F/W82A/I284F/T440Q}	
2a	100.00 ^b	408.25 ± 12.28	4.08
2b	5.79 ± 0.35	602.14 ± 24.65	104.00
2c	1.36 ± 0.63	311.70 ± 13.83	230.00
2d	0.94 ± 0.12	211.64 ± 14.55	224.75
2e	237.33 ± 11.21	616.25 ± 34.41	2.60
2f	350.84 ± 15.66	360.14 ± 9.32	1.03
2g	15.01 ± 2.31	65.48 ± 3.43	4.36
2h	10.91 ± 0.57	41.77 ± 1.83	3.83
2i	366.08 ± 13.21	520.05 ± 26.10	1.42
2j	689.14 ± 19.87	677.30 ± 35.52	0.98

^a The relative activity was determined from the initial reaction rate (*i.e.*, conversion <10%) relative to that of the WT enzyme. The reaction conditions were as follows: 15% DMSO, 50 mM acceptor, 250 mM L-Ala, and 2 μM purified enzyme in 100 mM Tris-HCl buffer (pH = 8.0) containing 0.1 mM PLP at 30 °C for 6 h; analyzed using HPLC. ^b The initial reaction rate was 0.9736 μM min⁻¹.

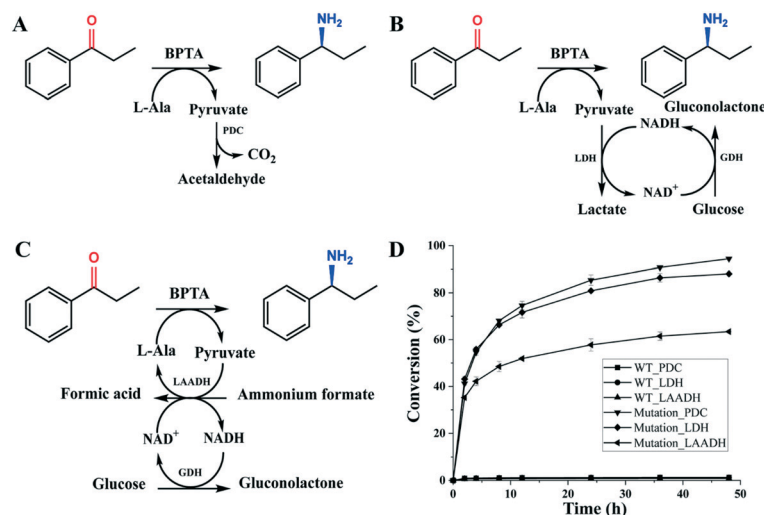


Fig. 3 Comparison of the asymmetric synthesis of (S)-1-amino-1-phenylpropane using the BPTAM78F/W82A/I284F/T440Q mutation and WT. (A)–(C) present the asymmetric synthesis of a chiral amine by ω -TA BPTA combined with the PDC, LDH and LAADH cascade reaction system, respectively. (D) Comparison of the conversion rates under various cascade reaction conditions by WT and the mutation M78F/W82A/I284F/T440Q.

systems with WT was inferior and showed no further obvious increase during the whole reaction after 4 h, and the highest conversion was only 1.3% at 48 h in the PDC cascade system. The conversion and reaction rates of the prochiral ketone catalyzed by the final variant BPTA_{M78F/W82A/I284F/T440Q} significantly improved. The conversion rates of the LDH and LAADH cascade reaction systems were 88.1% and 63.4%, respectively. The variant BPTA_{M78F/W82A/I284F/T440Q} combined with the PDC reaction system showed a comparatively higher conversion of 94.4% at 48 h. This result showed that the quadruple mutant BPTA_{M78F/W82A/I284F/T440Q} indeed conspicuously improved the catalytic efficiency for the asymmetric synthesis of a chiral amine compared with WT.

The reduction of substrate ketone **2b** was conducted using the mutant W82A/M78F/I284F/T440Q and PDC coupling cascade system at a substrate concentration of 10 mM on a 100 mL scale for 48 h at 30 °C. The reaction mixture was extracted and evaporated achieving 88.6% yield. The compound was characterized by ¹H NMR ((400 MHz, chloroform-*d*) δ 7.29–7.22 (m, 4H), 7.19–7.15 (m, 1H), 3.73 (t, *J* = 6.9 Hz, 1H), 1.63 (m, 2H), 1.54 (br, 2H), 0.80 (t, *J* = 7.4 Hz, 3H)) (Fig. S7†), and ¹³C NMR spectroscopy ((100 MHz, chloroform-*d*) δ 146.5, 128.5 (2C), 127.0, 126.5 (2C), 57.9, 32.5, 11.1) (Fig. S8†). The enantioselective analysis was carried out by HPLC, and the result is shown in Fig. S9†. We could observe only one peak at 37.20 min in the chiral HPLC, demonstrating the high stereoselectivity (up to >99.9% enantiomeric excess).

Conclusions

In this study, we rationally engineered an (S)-selective ω -transaminase BPTA to effectively synthesize the bulky aryl alkyl chiral amine (S)-1-amino-1-phenylpropane, which is not accommodated by selected natural transaminases. The

results of our mutation experiment showed that W82A plays a key role in relieving the steric barrier to accept and catalyze the target aryl alkyl ketone, 1-propionophenone, and M78F, I284F, and T440Q play an important role in improving the binding affinity and generation of the classical productive conformation in the active site. The rational engineering of the LBP successfully accommodated aryl alkyl substrates with bulkier small substituents, which are generally located in the SBP, and the utility of the asymmetric synthesis of chiral bulky amines was significantly improved relative to WT without any stereoselectivity loss. The rational engineering approach adopted in this study could potentially facilitate active site engineering to create an ω -transaminase variant that can accommodate structurally diverse substrates.

Experimental

Chemicals

(S)- α -Methylbenzylamine, (S)-phenylpropylamine, (S)-2-methyl-1-phenyl-1-propanamine, (S)-1-phenylbutan-1-amine, (S)-1-(4-methylphenyl)ethylamine, (S)-(-)-1-(4-methoxyphenyl)ethylamine, (S)-(+)-1-aminoindane, (S)-1,2,3,4-tetrahydro-1-naphthalenamine, (S)-(-)-1-methyl-3-phenylpropylamine, (S)-1-phenoxypropan-2-amine, phenoxyacetone, 4-phenylbutanone, acetophenone, propionophenone, isobutyrophenone, butyrophenone, 4'-methylacetophenone, 4'-methoxyacetophenone, 1-indanone, 1-tetralone, and pyridoxal 5-phosphate hydrate (PLP) were purchased from Sigma-Aldrich (St. Louis, USA). Other reagents used in this study were commercially available.

Mutagenesis, overexpression, and purification

An ω -transaminase BPTA (Gene ID: CP001044.1, <https://www.ncbi.nlm.nih.gov/nucleotide>) cloned from *Burkholderia phymatum* STM815 was ligated into the pET28a (+) expression vector by double digestion with the *Ned I* and *Hind III* restriction

enzymes (Thermo Fisher Scientific, USA) and transformed into *Escherichia coli* BL21 (DE3) cells (Thermo Fisher Scientific, USA). The single point mutation of BPTA was carried out using a QuickChange Lightning site-directed mutagenesis kit (Agilent Technologies Co.), according to the manufacturer's instructions.¹⁷ The primers for the mutation (Table S1†) were designed using the primer design program of Agilent (<http://www.agilent.com>). The amplicons were generated by PCR under the following thermal cycling conditions: 3 min at 95 °C, followed by 35 cycles at 95 °C for 15 s, annealing at 55 °C for 20 s, extension at 72 °C for 6 min, and a final extension step at 72 °C for 10 min. The amplicons were pooled and extracted using a FavorPrep™ GEL/PCR purification kit (Favorgen Biotech Corp., Taiwan). The mutagenesis was confirmed by DNA sequencing by Sangon Biotech.

We used lysogeny broth (LB) containing 50 µg mL⁻¹ kanamycin for the BPTA overexpression culture, incubating overnight for 12 h at 37 °C with shaking at 200 rpm. When the OD₆₀₀ reached 0.6, isopropyl-β-D-thiogalactoside (IPTG) was added to the culture at a final concentration of 0.1 mM, followed by further incubation for 20 h at 20 °C with shaking at 200 rpm. The culture broth was centrifuged at 10 000g for 20 min at 4 °C to pellet the cells, which were then resuspended in Tris-HCl buffer (pH = 8.0, 20 mM, containing 0.1 mM PLP). The pellets were disrupted by ultrasonication at 4 °C, and then centrifuged at 13 000g for 30 min at 4 °C to harvest crude enzymes in the supernatant.

The His-tagged BPTA enzyme purification was carried out using an AKTA Explore 100 system (GE Healthcare, USA) using a His-trap column (GE Healthcare) eluted with a linear gradient of imidazole (ranging between 10 mM and 0.5 M). The purified enzymes were concentrated and desalted using ultrafiltration (Millipore Co., Billerica, USA). The resulting samples were stored at -80 °C in 30% glycerol stock. The protein concentration was determined by the Bradford assay.⁴¹

Enzyme activity analysis

Unless otherwise specified, the BPTA enzyme assays towards (S)-1-amino-1-phenylpropane were all performed using an acetophenone photometric assay⁴² with slight modifications. The best determination wavelength for (S)-1-amino-1-phenylpropane and the corresponding ketone was ascertained by full wavelength scanning (Fig. S1†). The assay was performed at 30 °C for 10 min in a total of 200 µL (UV-Str 96-well plate, 655 801, Greiner Bio-one) containing 2.5 mM (S)-1-amino-1-phenylpropane (amino donor), 2.5 mM pyruvic acid (amino acceptor), and 15% DMSO. The production of 1-propionophenone was determined at 242 nm. One unit of BPTA enzyme activity was defined as the amount of enzyme that converted 1 µmol of (S)-1-amino-1-phenylpropane into acetophenone per minute.

Bioinformatic analysis

The models of WT and the variants were constructed by the searching algorithm of the Swiss modeling website ([\[swissmodel.expasy.org/\]\(http://swissmodel.expasy.org/\)\).⁴³ Molecular docking was carried out using the Autodock 4.2.6 suite software with the standard free-energy scoring function and the Lamarckian algorithm \(LGA\).¹⁶ The center of the grid box was defined in the N atom of the amino group in the PMP cofactor. The number of runs of LGA for the substrate ketone \(1-propionophenone\) and enzyme \(BPTA\) was 200. The population was set to 150, the maximum number of energy evaluations was 2 500 000, and the maximum number of generations was 27 000. The molecular dynamics simulation was carried out using Amber 16 with GAFF and the ff99SB force field, and the docking complex was placed in a solvated box using the TIP3PBOX model with a spacing distance of 10 Å. Counter ions were added to neutralize the charge in the solvated complex system. Two energy minimizations were performed first, followed by the NVT and NPT ensemble using Langevin dynamics.⁴⁴](http://</p>
</div>
<div data-bbox=)

Kinetic analysis

The kinetic parameters of WT and the variants towards (S)-1-amino-1-phenylpropane were obtained according to a pseudo kinetic model built with a fixed concentration of the co-substrate using the method of Lineweaver and Burk⁴⁵ with slight modifications. The *K_M* and *k_{cat}* values were calculated from the slopes and y-intercepts of the double reciprocal plots with various amine concentrations ranging between 0.1 and 2.5 mM. The purified enzymes were saturated with 0.1 mM PLP during purification.

Substrate specificity

The effects of various amino donors were investigated (Scheme 2). The reaction conditions were as follows: 15% DMSO, 50 mM (S)-amine, and 50 mM pyruvic acid in 100 mM Tris-HCl buffer (pH = 8.0) containing 0.1 mM PLP at 30 °C for 10 min; analyzed using HPLC. Similarly, to assess the spectrum of the acceptor, the following reaction conditions were used to determine the activities: 15% DMSO, 50 mM ketone, and 250 mM L-Ala (L-alanine) in 100 mM Tris-HCl buffer (pH = 8.0) containing 0.1 mM PLP at 30 °C for 6 h; analyzed using HPLC. All assays were performed in triplicate.

Asymmetric synthesis of (S)-1-amino-1-phenylpropane

To improve the reaction efficiency for the asymmetric synthesis of (S)-1-amino-1-phenylpropane, different cascade reaction systems were investigated. Reaction conditions 1: 10 mM 1-propionophenone, 250 mM L-Ala, 0.25 g BPTA dry cell power, 0.125 g pyruvate decarboxylase (PDC) dry cell power, and 15% DMSO. Reaction conditions 2: 10 mM 1-propionophenone, 250 mM L-Ala, 0.25 g BPTA dry cell power, 0.125 g lactate dehydrogenase (LDH) dry cell power, 0.125 g glucose dehydrogenase (GDH), 0.25 mM NAD⁺, 0.25 g glucose, and 15% DMSO. Reaction conditions 3: 10 mM 1-propionophenone, 250 mM L-Ala, 0.25 g BPTA dry cell power, 0.125 g L-amino acid dehydrogenase (LAADH) dry cell power, 0.125 g glucose dehydrogenase (GDH), 0.25 mM NAD⁺, 0.25 g

glucose, 25 mM ammonium formate, and 15% DMSO. Three reactions were performed in 100 mM Tris-HCl buffer (pH = 8.0) containing 1 mM PLP in a total volume of 10 mL at 30 °C for 48 h at 250 rpm. The 100 mL preparation scale conditions were as follows: 10 mM 1-propiophenone, 250 mM L-Ala, 2.5 g BPTA dry cell power, 1.25 g pyruvate decarboxylase (PDC) dry cell power, and 15% DMSO, and the reaction time was 48 h at 30 °C. After the reaction was completed, the pH of the mixture was adjusted to 3 to dissolve (S)-1-amino-1-phenylpropane as much as possible, and then the mixture was extracted with ethyl acetate three times. After the extraction, the pH of the mixture was adjusted to 13 to dissolve the ketones, and amine (S)-1-amino-1-phenylpropane was extracted three times with ethyl acetate. Finally, the extractions were collected and evaporated under vacuum at 40 °C to obtain the purified amine. The compound was analyzed using enantioselective analysis, as well as ^1H NMR and ^{13}C NMR spectroscopy.

HPLC analysis

HPLC analyses were carried out on an Agilent 1290 U-HPLC system equipped with a ZORBAX SB-AQ C18 column (4.6 × 250 mm × 5 µm) (Agilent Technologies Co., USA), heated to 37 °C using various ratios of methanol and water containing 0.1% trifluoroacetic acid (TFA) at 1 mL min⁻¹. The UV detection was performed at 210 nm. The details of the elution conditions are described in Table S2.† The quantitative chiral analyses of the amine products were performed using a CROWNPAK CR (+) column (4.6 × 150 mm × 5 µm) (Daicel Co., Japan), heated to 25 °C with 90% HClO₄ (pH = 1.5) and 10% methanol at a flow rate of 1 mL min⁻¹. The peak signal was detected by UV spectrophotometry at 220 nm.

Conflicts of interest

There are no conflicts to declare.

Acknowledgements

This work was supported by the National Natural Science Foundation of China (No. 21776084 and 22078097) and the Fundamental Research Funds for the Central Universities.

Notes and references

- 1 Z. S. Seddigi, M. S. Malik, S. A. Ahmed, A. O. Babalghith and A. Kamal, *Coord. Chem. Rev.*, 2017, **348**, 54–70.
- 2 A. Yohannes, X. Feng and S. Yao, *J. Chromatogr. A*, 2020, **1627**, 461395.
- 3 S. A. Kelly, S. Pohle, S. Wharry, S. Mix, C. C. R. Allen, T. S. Moody and B. F. Gilmore, *Chem. Rev.*, 2018, **118**, 349–367.
- 4 S. Wenda, S. Illner, A. Mell and U. Kragl, *Green Chem.*, 2011, **13**, 3007–3047.
- 5 J. F. Rocha, A. F. Pina, S. F. Sousa and N. M. Cerqueira, *Catal. Sci. Technol.*, 2019, **9**, 4864–4876.
- 6 M. Truppo, J. M. Janey, B. Grau, K. Morley, S. Pollack, G. Hughes and I. Davies, *Catal. Sci. Technol.*, 2012, **2**, 1556–1559.
- 7 P. P. Taylor, D. P. Pantaleone, R. F. Senkpeil and I. G. Fotheringham, *Trends Biotechnol.*, 1998, **16**, 412–418.
- 8 M. S. Malik, E.-S. Park and J.-S. Shin, *Appl. Microbiol. Biotechnol.*, 2012, **94**, 1163–1171.
- 9 F. Dumeignil, M. Guehl, A. Gimbernat, M. Capron, N. L. Ferreira, R. Froidevaux, J.-S. Girardon, R. Wojcieszak, P. Dhulster and D. Delcroix, *Catal. Sci. Technol.*, 2018, **8**, 5708–5734.
- 10 Á. Mourelle-Insua, D. Méndez-Sánchez, J. L. Galman, I. Slabu, N. J. Turner, V. Gotor-Fernández and I. Lavandera, *Catal. Sci. Technol.*, 2019, **9**, 4083–4090.
- 11 F. Guo and P. Berglund, *Green Chem.*, 2017, **19**, 333–360.
- 12 A. Nobili, F. Steffen-Munsberg, H. Kohls, I. Trentin, C. Schulzke, M. Höhne and U. T. Bornscheuer, *ChemCatChem*, 2015, **7**, 757–760.
- 13 M. Voss, D. Das, M. Genz, A. Kumar, N. Kulkarni, J. Kustos, P. Kumar, U. T. Bornscheuer and M. Höhne, *ACS Catal.*, 2018, **8**, 11524–11533.
- 14 C. K. Savile, J. M. Janey, E. C. Mundorff, J. C. Moore, S. Tam, W. R. Jarvis, J. C. Colbeck, A. Krebber, F. J. Fleitz, J. Brands, P. N. Devine, G. W. Huisman and G. J. Hughes, *Science*, 2010, **329**, 305–309.
- 15 I. V. Pavlidis, M. S. Weiss, M. Genz, P. Spurr, S. P. Hanlon, B. Wirz, H. Iding and U. T. Bornscheuer, *Nat. Chem.*, 2016, **8**, 1076–1082.
- 16 D. F. Dourado, S. Pohle, A. T. Carvalho, D. S. Dheeman, J. M. Caswell, T. Skvortsov, I. Miskelly, R. T. Brown, D. J. Quinn and C. C. Allen, *ACS Catal.*, 2016, **6**, 7749–7759.
- 17 K. S. Midelfort, R. Kumar, S. Han, M. J. Karmilowicz, K. McConnell, D. K. Gehlhaar, A. Mistry, J. S. Chang, M. Anderson, A. Villalobos, J. Minshull, S. Govindarajan and J. W. Wong, *Protein Eng., Des. Sel.*, 2013, **26**, 25–33.
- 18 S. W. Han, E. S. Park, J. Y. Dong and J. S. Shin, *Adv. Synth. Catal.*, 2015, **357**, 2712–2720.
- 19 E. S. Park, S. R. Park, S. W. Han, J. Y. Dong and J. S. Shin, *Adv. Synth. Catal.*, 2014, **356**, 212–220.
- 20 K. S. Midelfort, R. Kumar, S. Han, M. J. Karmilowicz, K. McConnell, D. K. Gehlhaar, A. Mistry, J. S. Chang, M. Anderson and A. Villalobos, *Protein Eng., Des. Sel.*, 2013, **26**, 25–33.
- 21 A. Nobili, F. Steffen-Munsberg, H. Kohls, I. Trentin, C. Schulzke, M. Höhne and U. T. Bornscheuer, *ChemCatChem*, 2015, **7**, 757–760.
- 22 M. Voss, D. Das, M. Genz, A. Kumar, N. Kulkarni, J. Kustos, P. Kumar, U. T. Bornscheuer and M. Höhne, *ACS Catal.*, 2018, **8**, 11524–11533.
- 23 M. S. Weiß, I. V. Pavlidis, P. Spurr, S. P. Hanlon, B. Wirz, H. Iding and U. T. Bornscheuer, *Org. Biomol. Chem.*, 2016, **14**, 10249–10254.
- 24 M. S. Weiß, I. V. Pavlidis, P. Spurr, S. P. Hanlon, B. Wirz, H. Iding and U. T. Bornscheuer, *ChemBioChem*, 2017, **18**, 1022–1026.
- 25 S. W. Han, E. S. Park, J. Y. Dong and J. S. Shin, *Adv. Synth. Catal.*, 2015, **357**, 1732–1740.
- 26 F. Ruggieri, J. C. Campillo-Brocal, S. Chen, M. S. Humble, B. Walse, D. T. Logan and P. Berglund, *Sci. Rep.*, 2019, **9**, 16946.

- 27 K. E. Cassimjee, B. Manta and F. Himo, *Org. Biomol. Chem.*, 2015, **13**, 8453–8464.
- 28 J.-S. Shin and B.-G. Kim, *Biosci., Biotechnol., Biochem.*, 2001, **65**, 1782–1788.
- 29 A. Dawood, M. Weiß, C. Schulz, I. Pavlidis, H. Iding, R. de Souza and U. Bornscheuer, *ChemCatChem*, 2018, **10**, 3943–3949.
- 30 B. Manta, K. E. Cassimjee and F. Himo, *ACS Omega*, 2017, **2**, 890–898.
- 31 K. Hirotsu, M. Goto, A. Okamoto and I. Miyahara, *Chem. Rec.*, 2005, **5**, 160–172.
- 32 J. Kyte and R. F. Doolittle, *J. Mol. Biol.*, 1982, **157**, 105–132.
- 33 Y. Westermaier, S. Ruiz-Carmona, I. Theret, F. Perron-Sierra, G. Poissonnet, C. Dacquet, J. A. Boutin, P. Ducrot and X. Barril, *J. Comput.-Aided Mol. Des.*, 2017, **7**, 757–760.
- 34 B.-K. Cho, H.-Y. Park, J.-H. Seo, J. Kim, T.-J. Kang, B.-S. Lee and B.-G. Kim, *Biotechnol. Bioeng.*, 2008, **99**, 275–284.
- 35 M. Genz, C. Vickers, T. Van Den Bergh, H.-J. Joosten, M. Dörr, M. Höhne and U. Bornscheuer, *Int. J. Mol. Sci.*, 2015, **16**, 26953–26963.
- 36 X. Robert and P. Gouet, *Nucleic Acids Res.*, 2014, **42**, W320–W324.
- 37 I. Slabu, J. L. Galman, R. C. Lloyd and N. J. Turner, *ACS Catal.*, 2017, **7**, 8263–8284.
- 38 T. Börner, G. Rehn, C. Grey and P. Adlercreutz, *Org. Process Res. Dev.*, 2015, **19**, 793–799.
- 39 D. Koszelewski, K. Tauber, K. Faber and W. Kroutil, *Trends Biotechnol.*, 2010, **28**, 324–332.
- 40 M. Hoehne, S. Kuehl, K. Robins and U. T. Bornscheuer, *ChemBioChem*, 2008, **9**, 363–365.
- 41 M. M. Bradford, *Anal. Biochem.*, 1976, **72**, 248–254.
- 42 S. Schätzle, M. Höhne, E. Redestad, K. Robins and U. T. Bornscheuer, *Anal. Chem.*, 2009, **81**, 8244–8248.
- 43 T. Schwede, J. Kopp, N. Guex and M. C. Peitsch, *Nucleic Acids Res.*, 2003, **31**, 3381–3385.
- 44 S.-W. Han, J. Kim, H.-S. Cho and J.-S. Shin, *ACS Catal.*, 2017, **7**, 3752–3762.
- 45 H. Lineweaver and D. Burk, *J. Am. Chem. Soc.*, 1934, **56**, 658–666.